

Feasibility study on in-situ heat injection of Tongchuan oil shale and tar-rich coal based on TG-DTG

Heping YAN^{1*}, Xiurong WU², Qiang LI³, Yinghui FANG², and Qingfeng BU^{3**}

¹ School of Resources and Geosciences, China University of Mining and Technology, Xuzhou, 221116, China

² Shaanxi 194 Coal Geological Co., Ltd., Tongchuan 727007, China

³ College of Construction Engineering, Jilin University, Changchun 130026, China

Abstract. In-situ thermal injection is an effective development method for low-value unconventional resources. The nonisothermal pyrolysis characteristics of Tongchuan oil shale and tar-rich coal were investigated by TG-DTG extrapolation. In addition, the pyrolyzed shale oil was analyzed. The results show that the pyrolysis of oil shale and tar-rich coal can be divided into three stages. The pyrolysis temperature intervals of both can be consistent. Compared with the oil shale, the ignition temperature of the mix decreased by 2.3%, and the burnout temperature increased by 1.4%. The pyrolysis index increased by 40.3%, the pyrolysis stability increased by 66.7%, and the content of oxygenated compounds increased by 552.4%. The conversion of oxygenated compounds to phenolic compounds was inhibited at the 20°C/min heating rate. In the air, the excessively fast heating rate caused the tar to condense earlier and coke on the sample surface. The pyrolysis index of the mix decreased from 3.2 to 1.8 times, while the pyrolysis stability increased by 6.7 times, respectively. The introduction of excessive oxygenated groups by the air increased the content of oxygenated compounds in the mix by 485.44% while the aromatic hydrocarbons decreased by 17.97%. It can be seen that the co-pyrolysis of oil shale and tar-rich coal can improve the ignition characteristics of oil shale. The co-pyrolysis of oil shale and tar-rich coal not only conforms to the distribution characteristics of both but also greatly cooperates with the topical chemical reaction method.

Keywords: in-situ conversion; Tongchuan oil shale; TG-DTG; pyrolysis characteristics.

1. INTRODUCTION

China's energy structure is characterized as "rich in coal, poor in oil, and low in gas." The country's insufficient oil and gas supply and demand is exacerbated by the country's rapid economic expansion [1]. Hydrocarbons can be produced by pyrolyzing the solid organic materials in oil shale at high temperatures [2, 3]. Tar-rich coal contains significant levels of tar (7% to 12%), which can be pyrolyzed at high temperatures to release hydrocarbon compounds [4–6]. The majority of oil shale in China is produced from continental deposits. During the deposition process, buoyancy drives the formation of oil shale reservoirs, which possess complex pore structures and often accumulate oil and gas within the reservoir or in near-source accumulations [7–11]. This uneven distribution of oil shale resource grades is a result of the geological processes. Additionally, coal and oil shale deposits are interconnected, with tar-rich coal seams often occurring above or below oil shale [12] like, for example, in Tongchuan City in China Shaanxi Province.

Numerous academics studied the co-pyrolysis of coal and oil shale to achieve hydrogen transfer and create a synergistic effect that will increase production [13, 14]. Miao *et al.* [15] selected coal samples from various mining areas for co-pyrolysis with oil

shale. The results indicated that, at the same mixing ratio, low-rank coal with high volatile matter, low moisture, and low ash content was more likely to produce a synergistic effect with oil shale, whereas co-pyrolysis of high-moisture coal and oil shale was less favourable for achieving this effect. Dong *et al.* [16] investigated the co-pyrolysis properties of coal and oil shale using microwave heating. They also examined the composition distribution at various mixture ratios and the yield of pyrolysis products. The results revealed that microwave pyrolysis increased both the tar yield and the amounts of combustible gases in the produced gas. Chun *et al.* [17] studied the effects of different oil shale blending ratios on the pyrolysis properties and gas composition of the co-pyrolysis process, using TG-FTIR, by mixing oil shale with bituminous coal and lignite in an inert environment. The findings showed a synergistic effect between the two pyrolysis processes and an increase in the liquid and gas products when the oil shale content was 50%. However, bituminous coal hindered the pyrolysis of oil shale during their co-pyrolysis. Murat *et al.* [18] investigated the pyrolysis properties of co-pyrolysis using lignite combined with two oil shales in a fixed-bed reactor. The results demonstrated a strong synergistic effect between lignite and oil shale, along with an improvement in the yield and quality of tar as the oil shale blending ratio increased.

Therefore, co-pyrolysis of different types of coal and oil shale can improve oil and gas production. However, tar-rich coal and oil shale contain hydrocarbon components, if co-pyrolysis of both will generate a synergistic effect does not have relevant research results.

e-mail: * yijiusiduiyonghebu@163.com

** buqf22@mails.jlu.edu.cn

Manuscript submitted 2024-08-25, revised 2025-02-25, initially accepted for publication 2025-03-25, published in July 2025.

Thermogravimetric-differential scanning calorimetry (TG-DSC) provides comprehensive insights into overall reaction kinetics. This method has been widely used to study the isothermal and nonisothermal pyrolysis properties of fossil fuels [19–21]. The kinetics of oil shale pyrolysis were investigated using TG-DTG, which effectively explained the relationship between maturity and the temperature distribution during oil shale pyrolysis [22]. Bao [23] conducted a comprehensive study of enhanced recovery technologies over the past decade. Molecular diffusion was examined as a key mechanism in seepage and oil recovery through empirical correlations and experimental measurements. Sun *et al.* [24] investigated the pyrolysis kinetics of multi-stage parallel reactions of Huadian oil shale at various heating rates and particle sizes. The results indicated that increasing particle size or heating rate shifted the combustion process to higher temperatures due to mass transfer resistance and thermal lag. Both oil shale and tar-rich coal are unconventional oil and gas resources with low oil content, making them valuable for development only if the economic investment cost is low [25]. Therefore, understanding the relationship between the pyrolysis characteristics and segments of oil shale and tar-rich coal under varying atmospheric conditions and heating rates is crucial for achieving in situ thermal injection mining and enhancing oil and gas recovery.

The technique of triggering in-situ pyrolysis of oil shale through topo-chemical reactions is a complex chemical process [26]. In the initial stage, solid organic matter pyrolysis is induced by introducing high-temperature nitrogen. Subsequently, the nitrogen is replaced with air to further promote the decomposition of solid organic matter [27]. Oxidation reactions release large amounts of heat and continuously accelerate the pyrolysis of oil shale during its formation [28]. The source of combustion in the oxidation reaction is the fixed carbon in the oil shale. A low concentration of fixed carbon cannot initiate a topo-chemical reaction. The high carbon content in tar-rich coal compensates for the inadequately fixed carbon in oil shale. Therefore, this paper takes the geological characteristics in Tongchuan as the research object, adopts the TG-DTG extrapolation method and low-temperature dry distillation experiments to study the pyrolysis characteristics and pyrolysis oil of oil shale and tar-rich coal, exploring the pyrolysis characteristics of the co-pyrolysis and the distribution characteristics of the oil products in different pyrolysis atmospheres. The results of this study provide technical support for exploring the feasibility of in-situ heat injection of oil shale and tar-rich coal in Tongchuan.

2. MATERIAL AND METHODS

2.1. Material

Tongchuan oil shale used in the experiments was sourced from a depth of 150–200 m in the Jiaoping coal mine, located in the Ordos Basin, with a sedimentary thickness of 10–15 m. The upper layer consists of siltstone deposits, while the lower layer is composed of grey mudstone. The tar-rich coal was also sourced from the Jiaoping mining area, buried at a depth of 160–300 m with an average thickness of 10.4 m. It is primarily composed

of semi-bright and semi-dark coals, interspersed with lumpy structures. The fracture density in the coal seam ranges from 5 to 50 per 5 cm.

The samples were ground and sieved to approximately 80 mesh before testing. Then, they were placed in a constant-temperature drying oven, dried at 80°C until reaching a constant weight, and subsequently sealed for storage. The results of proximate and element analyses of the oil shale are presented in Table 1.

Table 1

Analysis of oil shale and tar-rich coal

Attribute region	Proximate analysis (wt. %)				
	Moisture	Ash	Volatiles	Fixed carbon	
Oil shale	0.86	78.22	18.14	2.78	
Tar-rich coal	5.45	5.60	41.50	47.45	
Attribute region	Element analysis (wt.c%)				
	H	C	N	S	O
Oil shale	3.18	9.22	0.72	0.29	0.36
Tar-rich coal	5.36	77.42	1.52	0.42	15.28

The experiment was divided into three groups: (1) oil shale, (2) tar-rich coal, and (3) a homogeneous mixture of both, with each component comprising 50% of the mixture. To facilitate discussion, these groups are referred to as T₁, T₂, and T₃, respectively.

Dry distillation tests for T₁, T₂, and T₃ were conducted using a DC-GJ-4 dry distillation furnace. Each sample weighed 80 g. The heating rate was set at 5°C/min, with the temperature gradually increasing from 25 to 600°C, followed by a 30-minute hold at the final temperature.

The experiment generated liquid oil, pyrolysis water, and solid residue. The liquid oil was then analyzed using GC-MS. The dry distillation results of oil shale and tar-rich coal are presented in Table 2.

Table 2

Result of cryogenic dry distillation test

Region	Tar (wt.%)	Total moisture (wt.%)	Semicoke (wt.%)	Gas + loss (wt.%)
Oil shale	5.48	9.06	82.81	2.65
Tar-rich coal	10.65	6.54	73.46	9.35

2.2. Method

The TG-DTG analysis of the co-pyrolysis and product release characteristics of oil shale and tar-rich coal is crucial for assessing the feasibility of in-situ co-pyrolysis in Tongchuan and optimizing crude oil production. It aids in understanding how different pyrolysis atmospheres affect key characteristics, such as in-situ pyrolysis temperatures and pyrolysis stability.

Feasibility study on in-situ heat injection of Tongchuan oil shale and tar-rich coal based on TG-DTG

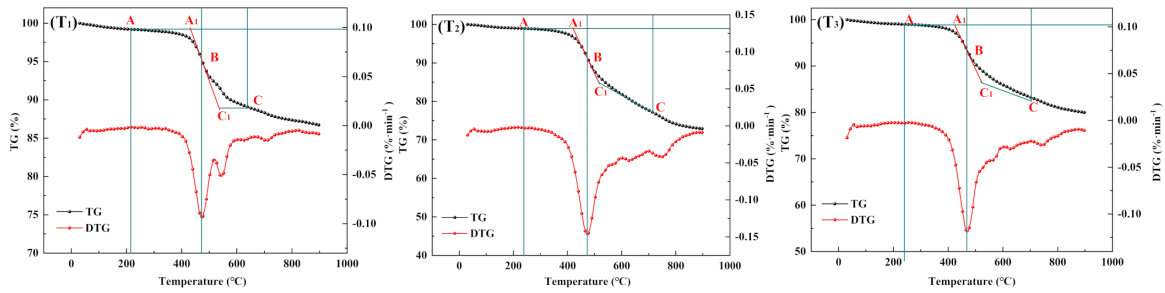


Fig. 1. The experimental group for extrapolation calibration under nitrogen atmosphere (20°C/min)

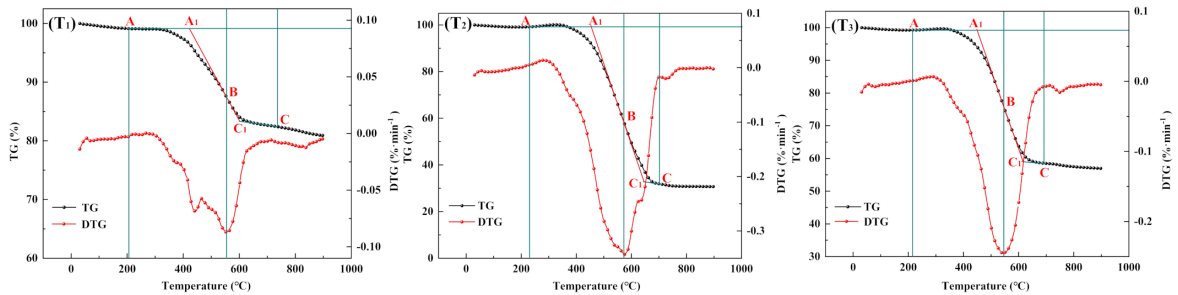


Fig. 2. The experimental group for extrapolation calibration under air atmosphere (20°C/min)

2.2.1. Pyrolysis characterization parameters

Using the TG-DTG extrapolation method, the initial pyrolysis temperature can be determined by analyzing the TG-DTG curve [29]. The DTG curve shows that the weight loss rate is highest at point B, which vertically intersects the TG curve.

The tangent to the TG curve at point B intersects the extended line from the initial point A of the TG curve at point A₁. This intersection represents the temperature corresponding to the ignition point of the oil shale. After reaching the maximum weight loss rate, the DTG curve shows a steady decrease at point C, which marks the end of the second stage on the TG curve. The tangent line at point B intersects at point C₁, which represents the final pyrolysis temperature of the organic matter. The pyrolysis interval diagrams for Tongchuan oil shale, tar-rich coal, and their mixture, under nitrogen and air conditions, were determined through extrapolation and are presented in Fig. 1 and Fig. 2.

2.2.2. Pyrolytic stability analysis

Using the measured data for pure carbon and the TG-DTG curves from the experiments, pyrolysis stability was compared using the pyrolysis index C , the pyrolysis stability S and comprehensive pyrolysis index R_w [30].

$$C = \frac{(d_m/d_t)_{\max}}{T_i^2}, \quad (1)$$

$$R_w = \frac{655}{T_i} \times \frac{763}{T_{\max}} \times \frac{(d_m/d_t)_{\max}}{0.00582}, \quad (2)$$

where T_i is the initial pyrolysis temperature, °C; $(d_m/d_t)_{\max}$ is the maximum weight loss rate, %/min; 655 is the ignition point

of pure carbon, °C; 763 is the temperature corresponding to the maximum weight loss rate (0.00582) of pure carbon, °C; and T_{\max} is the corresponding temperature of the maximum weight loss rate, °C.

$$S = \frac{(d_m/d_t)_{\max} (d_m/d_t)_{\text{mean}}}{T_i^2 T_c}, \quad (3)$$

$$\left(\frac{d_m}{d_t}\right)_{\text{mean}} = \frac{(d_m/d_t)_i (d_m/d_t)_c}{2}, \quad (4)$$

where T_c is the burnout temperature, °C; $(d_m/d_t)_i$ is the pyrolysis rate of ignition point, %/min; $(d_m/d_t)_c$ is the pyrolysis rate of burnout temperature, %/min.

2.2.3. Release characteristics of products

The degree of product release concentration r characterizes the pyrolysis product release properties and differences between experimental groups under nonisothermal conditions. In this paper, the release characteristics of pyrolysis products were calculated for the experiment with 50% and 75% conversion in the second stage.

$$\Delta T_{1/2} \rightarrow \frac{(d_m/d_t)}{(d_m/d_t)_{\max}} = \frac{1}{2}, \quad (5)$$

$$r_{1/2} = \frac{(d_m/d_t)_{\max}}{T_{\max} T_i \Delta T_{1/2}}, \quad (6)$$

$$\Delta T_{3/4} \rightarrow \frac{(d_m/d_t)}{(d_m/d_t)_{\max}} = \frac{3}{4}, \quad (7)$$

$$r_{3/4} = \frac{(d_m/d_t)_{\max}}{T_{\max} T_i \Delta T_{3/4}}, \quad (8)$$

where $\Delta T_{1/2}$ is the temperature range corresponding to 50% conversion, °C, also known as half peak width; $\Delta T_{3/4}$ is the temperature range corresponding to 75% conversion, °C; $r_{1/2}$ and $r_{3/4}$ denote the concentration of pyrolysis product release at 50% and 75% conversion, respectively.

3. RESULTS AND ANALYSIS

3.1. TG test result analysis

This study aims to evaluate in-situ heat injection mining of the interbedded oil shale and tar-rich coal strata in the Tongchuan area using the topo-chemical situ reaction method. To achieve this, nitrogen and air were used as the primary parameters for comparative analysis. TG analysis was conducted on Tongchuan oil shale (T_1), tar-rich coal (T_2), and both homogeneous mixture (T_3) at a heating rate of 20°C/min.

The maturity of the solid organic matter in the oil shale exhibits significant variation due to differences in the genesis environment. Consequently, the temperature intervals in the TG curves and the magnitude of weight loss differ. To more clearly demonstrate the relationship between the weight loss of Tongchuan oil shale and the pyrolysis interval during heating, and to facilitate comparison with previous research, the temperature curve is blurred to a certain extent here. For instance, the pyrolysis temperature range of 354°C~625°C is modified to 350°C~620°C.

As illustrated in Fig. 3, the pyrolysis of Tongchuan oil shale in nitrogen can be broadly divided into three stages. The first stage (25–300°C) primarily involves the drying and dehydration of the oil shale. The liquid water trapped in pore fractures starts to vaporize depending on the energy required. Following, the oil shale takes a dehydration reaction, releasing bound water from the rock structure. In the second stage (300–480°C), the solid organic matter begins to soften and undergo pyrolysis. This solid organic matter is treated as a large organic functional group with significant variability in maturity. The temperature required for the thermal evolution process varies. This stage represents the primary interval for hydrocarbon production. In the third stage (480–900°C), the weight loss rate stabilizes, indicating that the solid organic matter is fully pyrolyzed. A fluctuation in the TG

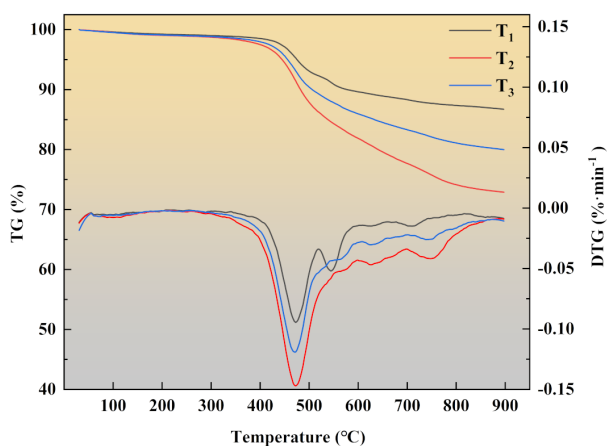


Fig. 3. TG-DTG curves of experiments in the nitrogen atmosphere

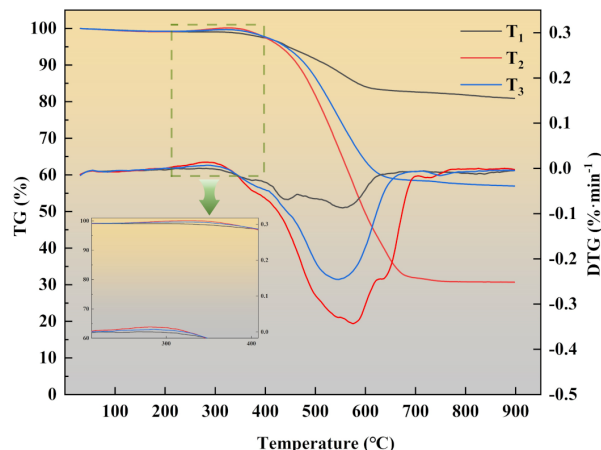


Fig. 4. TG-DTG curves of experiments in the air atmosphere

at 520°C is observed, likely due to the thermal decomposition of clay minerals.

Figures 3 and 4 represent the TG-DTG results of different experimental groups in the nitrogen and air atmospheres, respectively. The weight loss of T_2 is greater than T_1 in all cases. The weight loss of T_3 is in between. Tar-rich coals have a higher carbon content and are pyrolyzed to a greater extent in high-temperature environments. This phenomenon is more obvious as the pyrolysis temperature moves towards the high temperature. Comparing the maximum weight loss of T_3 in the different atmospheres, the weight loss of T_3 decreased from 80% to 60%. The presence of tar-rich coal prolongs the second stage of oil shale pyrolysis, which is the main hydrocarbon interval. The carbon-rich and porous structure of tar-rich coal extends the heating time, allowing both to be cracked to a higher degree and the heavy components to be cracked more fully. In particular, in the air atmosphere, oxygenated gases oxidize and exothermically react with the fixed carbon, resulting in a significant decrease in weight loss. It is important for triggering and maintaining topical chemical reactions.

The T_2 and T_3 curves show an ascending and then a descending trend in the 210–250°C temperature interval (shown in Fig. 4). This is the adsorption of coal for oxygen atoms in the air, and the more reactive hydroxyl and carboxyl groups in the coal skeleton, forming temporary chemical bonds and intermediates, which make the weight of the sample increase. With the increase in temperature, the oxidation reaction is enhanced and the coal starts to decompose [14]. Therefore, oil shale and tar-rich coal remain relatively consistent in the main pyrolysis temperature interval, which means that synchronized in-situ heat injection of both can be achieved.

3.2. Pyrolysis characterization

The TG-DTG curves for T_1 , T_2 , and T_3 were measured under both nitrogen and air at heating rates of 10°C/min and 20°C/min. The pyrolysis parameters were then derived through TG-DTG extrapolation, as detailed in Tables 3 and 4.

As discussed in Section 3.1, the first stage of the TG curve corresponds to the dehydration and weight loss of the sample.

Feasibility study on in-situ heat injection of Tongchuan oil shale and tar-rich coal based on TG-DTG

Table 3

Pyrolysis characteristics of the experiment under nitrogen

Region	Heating rate (°C/min)	T_o (°C)	T_i (°C)	T_{max} (°C)	$(d_m/d_t)_{max}$ (%/min)	T_c (°C)
T ₁	10	232	425	465	0.091	511
T ₂		207	416	462	0.143	520
T ₃		216	415	459	0.114	519
T ₁	20	234	438	472	0.095	520
T ₂		229	427	465	0.147	535
T ₃		232	428	470	0.119	527

Table 4

Pyrolytic characteristics of experiment under air

Region	Heating rate (°C/min)	T_o (°C)	T_i (°C)	T_{max} (°C)	$(d_m/d_t)_{max}$ (%/min)	T_c (°C)
T ₁	10	224	410	532	0.091	568
T ₂		207	439	526	0.493	586
T ₃		197	400	529	0.316	578
T ₁	20	227	418	555	0.087	601
T ₂		224	454	575	0.343	646
T ₃		214	409	546	0.246	614

Before reaching the ignition point, the dehydration rate is slow due to the sample water content being less than 4%. Once the ignition point is reached, the pyrolysis rate of the solid organic matter accelerates significantly, and the weight loss becomes more pronounced (Figs. 3 and 4). As shown in Table 3, the ignition temperature of T₃ is significantly lower than that of T₁, with a decrease of about 2.3%, and the burnout temperature of T₃ increases by about 1.4%, which contributes to the in-situ heat injection. This phenomenon does not change as the heating rate increases, and the experimental sample temperature is transferred mainly by convective heat transfer in the nitrogen atmosphere. This transfer process is simply physical, and the free hydrocarbons and tars contained within the sample are removed from the sample with the experimental circulating medium without combustion [31].

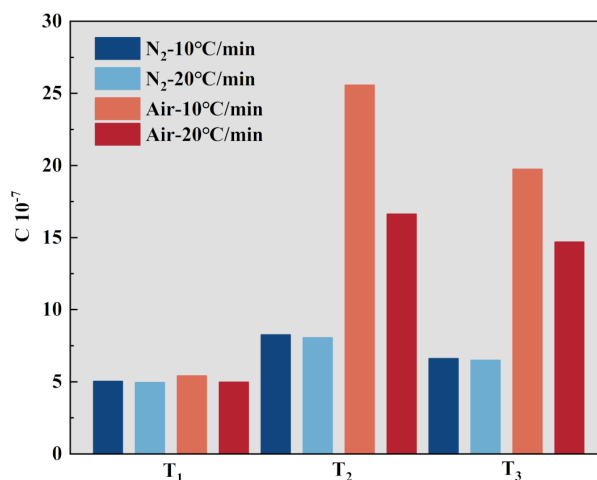
As shown in Table 4, the ignition temperature of T₁ decreases by 15–20°C and the ignition temperature of T₂ increases by 23–27°C in comparison to the nitrogen atmosphere, which is mainly since the free hydrocarbons in the pores are favourable for the ignition of the sample as the pyrolysis temperature reaches 350°C. On the contrary, in the oxygenated gas atmosphere, a large amount of tar is adsorbed on the sample surface and coking, closing the pore space [32]. In addition, there is a significant relationship between the increase in burnout temperature and the heating rate, with a doubled heating rate resulting in a 36°C increase in burnout temperature. This situation is somewhat different from that in a nitrogen atmosphere, which is the result of

the concentration of oxygenated gas leading to an enhanced intensity of the oxidation reaction and an increase in the oxidative exothermic time [31].

It can be seen that the presence of tar-rich coal contributes to the improvement of the pyrolysis characteristics of oil shale in nitrogen and air atmospheres. This improvement is mainly expressed in two aspects. First, the high carbon content of tar-rich coal in the nitrogen atmosphere helps to provide sufficient combustibles, i.e., fixed carbon, with the initial triggering of topical chemical reactions. Second, both oil shale and tar-rich particles can be regarded as porous media, which provide a carrier for the full pyrolysis of tar, making the pyrolysis of tar more adequate, and avoiding the early condensation reaction between tar and solid organic matter in the oxygenated atmosphere, leading to coking of the samples or asphaltene blockage of the pores. In conclusion, the co-pyrolysis of oil shale and tar-rich coal can improve the ignition characteristics of both and increase the success probability of in-situ heat injection.

3.3. In-situ pyrolysis characterization

The pyrolysis index C , the pyrolysis stability S and comprehensive pyrolysis index R_w for the experiment under various atmospheres and heating rates are calculated, as illustrated in Figs. 5–7.

**Fig. 5.** Pyrolysis index C under different experimental conditions

The pyrolysis index C indicates the early pyrolysis performance of the experiment, specifically the ignition ability of oil shale and tar-rich coal in situ. As can be seen from Table 3, the ignition characteristics of T₁ are all maintained at a low level, which indicates that the oil shale has poor thermophysical properties as compared to T₂ and T₃. In previous studies [33], oil shale had low permeability and low calorific value, which determined the difficulty of triggering topical reactions in oil shale reservoirs. In the nitrogen atmosphere, the pyrolysis indices of T₂ and T₃ were greater than T₁ with an increase of 50% and 40%, respectively, and the structure of tar-rich coal was looser compared with oil shale, and the high-temperature environment promoted the pyrolysis of coal. This advantage becomes even greater in the air atmosphere. At 10°C/min, the pyrolysis indices

of T_2 and T_3 were 4.2 and 3.2 times that T_1 . The increase of pyrolysis index was about 2.4 and 1.8 times at $20^\circ\text{C}/\text{min}$, which was the result of fast heating rate that led to the early condensation of tar and coking on the samples surface resulting in the decrease of pyrolysis efficiency [34].

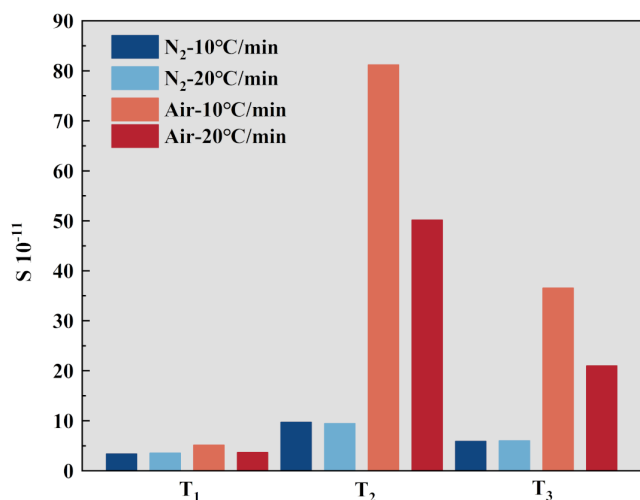


Fig. 6. Pyrolytic stability S under different experimental conditions

S represents the pyrolysis stability of T_1 , T_2 , and T_3 during pyrolysis, which is crucial for maintaining a continuous pyrolysis reaction in oil shale. From Fig. 6, the pyrolysis stability of T_1 is lowest. In particular, there is a greater feasibility of interrupting autonomous pyrolysis when higher flowrate of air is injected. On the contrary, the coal structure ensures more thermal stability. The pyrolytic stability of T_3 is enhanced by about 66% in nitrogen atmosphere and 6.7 times in air atmosphere with respect to T_1 , which indicates T_3 can significantly improve oil shale pyrolysis stability. This enhancement depend on the combustibility of coal and the oxidative exotherm reaction [35]. In addition, with the increase of heating rate, a large amount of asphalt in the tar-rich coal was rapidly generated and released, which led to a combustion reaction in which oxygenated gases could not come into contact with the combustible matter in the experiment. A large number of free radicals were generated by the breakage of bridge bonds during coal pyrolysis, and the heating rate was fast, which led to the early occurrence of the condensation reaction [36]. As a result, controlling injection parameters is significantly important for the continuity of in-situ heat injection [37]. When organic matter is excessively converted to coke or heavy tar, these accumulate in the reservoir, affecting the subsequent migration of light oil and gas [38].

Oil shale is a nonconventional energy source rich in ash and solid organic matter, making its pyrolysis challenging to achieve [39]. According to the extrapolation analysis results in Tables 3 and 4, T_2 outperforms T_1 in ignition point, burnout temperature, pyrolysis index C , and comprehensive pyrolysis index R_w (Figs. 5 and 7). Consequently, T_3 , with 50% tar-rich coal, exhibits a lower ignition point, higher burnout temperature, and improved, more stable pyrolysis characteristics. This indicates that Tongchuan oil shale and tar-rich coal can achieve

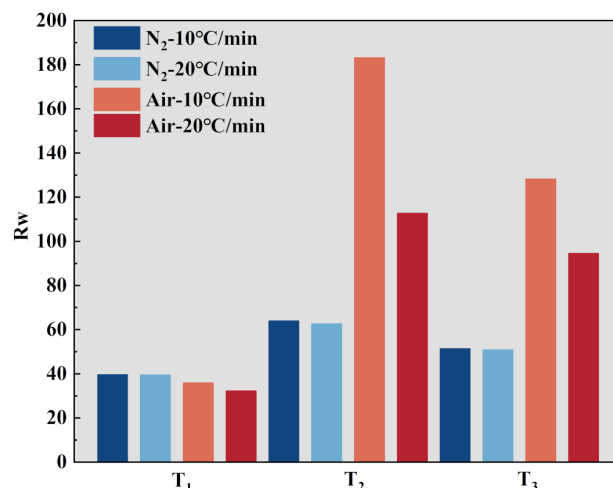


Fig. 7. Comprehensive pyrolysis index R_w under different experimental conditions

in-situ co-pyrolysis and maintain a more stable continuous pyrolysis reaction, indirectly enhancing the overall economic efficiency of in-situ pyrolysis. The comprehensive pyrolysis index R_w provides a more balanced view of the benefits of co-pyrolysis (Fig. 7), with these benefits being more pronounced in air. The in-situ pyrolysis of Tongchuan oil shale with tar-rich coal aligns well with the topo-chemical reaction method, significantly enhancing the likelihood of successful in-situ pyrolysis.

3.4. Pyrolysis product analysis

The GC-MS results of the pyrolysis products from T_1 , T_2 , and T_3 under both nitrogen and air are presented in Figs. 8 and 9.

A comparison of Fig. 8 (T_1) and (T_3) shows that during the co-pyrolysis of Tongchuan oil shale and tar-rich coal in the nitrogen atmosphere, the alkanes and olefins decreased significantly by 48.50% and 61.54%, respectively. The content of aromatic hydrocarbons and oxygenated compounds increased significantly by 7.73% and 552.41%, respectively. As the temperature rises, the long-chain aliphatic hydrocarbons in the sample is broken, generating short-chain aliphatic hydrocarbons and small-molecule aromatic hydrocarbons in the nitrogen atmosphere. Due to the low ignition point of aliphatic hydrocarbons, most of the aliphatic hydrocarbons are ignited to release a large amount of heat, which causes the breakage of oxygenated functional groups such as hydroxyl and carbonyl groups in the coal [40]. These free radicals continuously collide with the coal molecules, resulting in C-O bond breakage and generating large molecule fragments, which convert some of the fragments into tar [41]. At the rapid heating rate of $20^\circ\text{C}/\text{min}$, the conversion of oxygenated compounds to phenolic compounds is inhibited, which promotes the interactions between free radicals and weakens the occurrence of secondary cracking reaction [42]. Therefore, the oxygenated compounds in the resulting tar are significantly improved. It is shown that higher heating rates can reduce the extent of dehydroxylation, deoxygenation, and cleavage of long-chain aliphatic structures, which are favourable to the enhancement of oxygenated compounds as well as polar compounds [43, 44]. In

Feasibility study on in-situ heat injection of Tongchuan oil shale and tar-rich coal based on TG-DTG

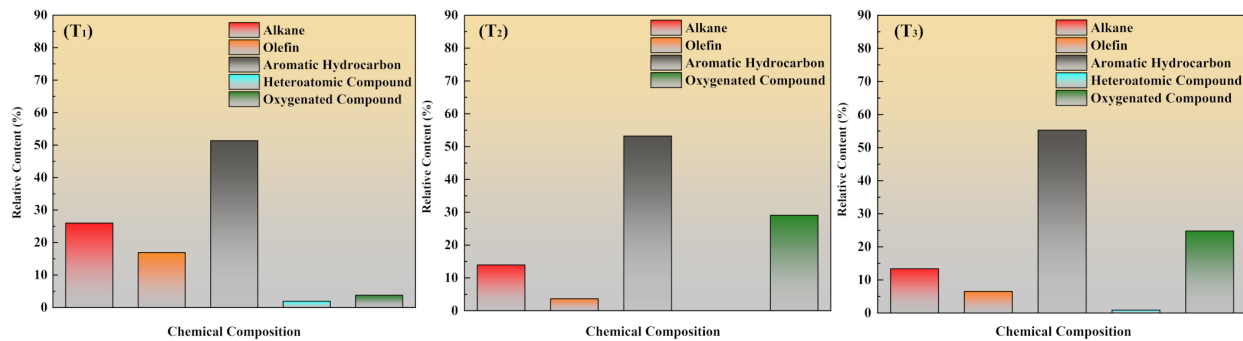


Fig. 8. GC-MS results of experiments under nitrogen

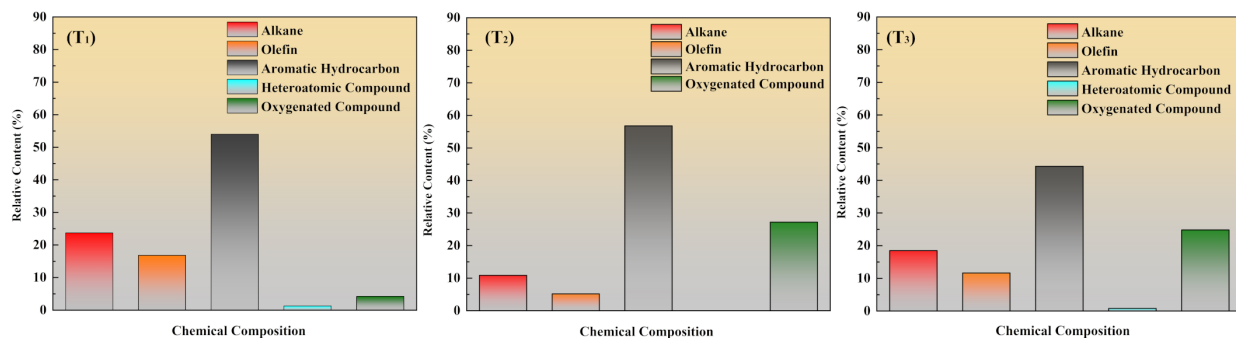


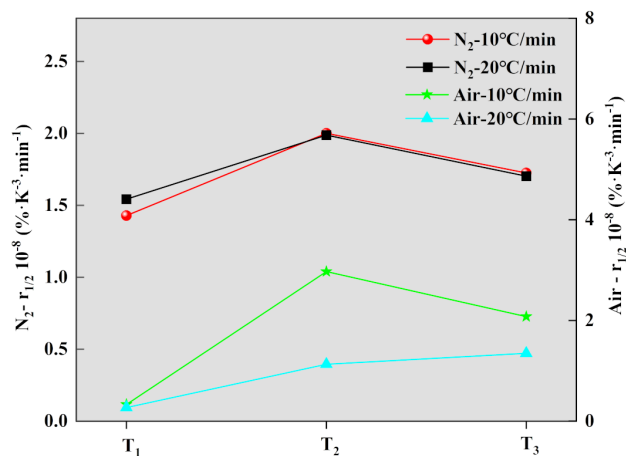
Fig. 9. GC-MS results of experiments under air

addition, the faster heating rate favours the polycondensation reaction, which is the main reason why the aromatic hydrocarbon contents of T₂ and T₃ remain relatively levelled [45].

As shown in Fig. 9, compared to T₁, the content of alkanes and olefins, decreases to 21.94% and 30.84%, respectively. The content of oxygenated compounds increases by 485.44%. It is noteworthy that aromatic hydrocarbons decrease by 17.97%. It is easily seen that the air atmosphere has a significant effect on the characterization of pyrolysis products in T₂ and T₃, and on the characterization of pyrolysis products in the experimental group. According to aerobic pyrolysis, the oxidation reaction makes aliphatic hydrocarbon groups, methyl groups, and other aliphatic groups, form a large number of oxidized free radicals, i.e., hydroxyl, carboxyl, aldehyde, and ether groups. These functional groups have much lower activation energies which make them highly accessible to exothermic reactions with oxygen [46]. It allows the solid organic matter and carbon skeleton inside the sample to be completely oxidized. Leading to secondary pyrolysis and cyclization of the pyrolysis products, short-chain aliphatic hydrocarbons and small aromatic hydrocarbons are produced. Some research [47,48] proves that aerobic pyrolysis reduces the recovery efficiency in the excessive oxygen content. In addition, with the increase in pyrolysis temperature, the oxygenated functional groups are easy to be removed by thermal pyrolysis at high temperatures, which should result in a decrease of oxygenated compounds and an increase of phenolic compounds. However, an increased trend in the content of oxygenated compounds in T₃ is observed, indicating that an excess of oxygenated groups is introduced for the pyrolysis reaction in

the air atmosphere. In pyrolysis, the oxygenated compounds consumed are lower than the oxygenated compounds produced [49].

As shown in Figs. 10 and 11, the product release characteristic $r_{1/2}$ in the nitrogen atmosphere is larger than that in the air atmosphere due to the dependence of the sample temperature on the convective heat transfer of the heat-carrying medium in the early period. Tar-rich coal is looser with better convective heat transfer and is not affected by heat transfer hysteresis. Therefore, the higher the content of tar-rich coal, the more concentrated the product release characteristic $r_{1/2}$. This phenomenon also appears in the product release characteristic $r_{3/4}$ curve. Moreover, the effect of heating rate on the product release characteristics

Fig. 10. $r_{1/2}$ with different pyrolysis conditions

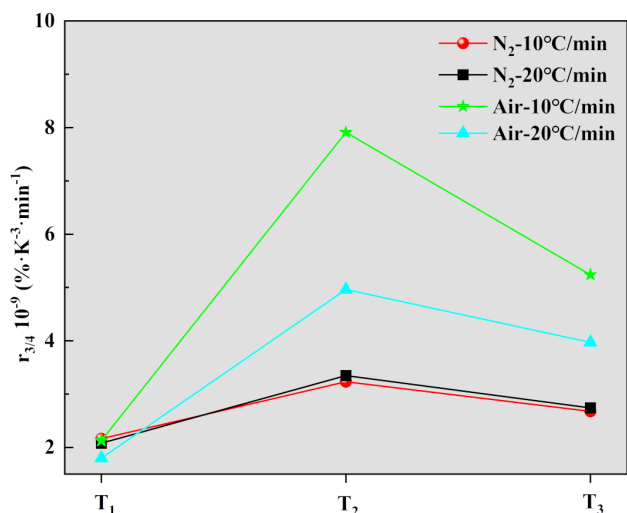


Fig. 11. $r_{3/4}$ with different pyrolysis conditions

is even more remarkable, which is more obvious in the air atmosphere. The $r_{1/2}$ and $r_{3/4}$ of T₃ are better than T₁, indicating that the presence of tar-rich coal contributes to the product release from oil shale in the pyrolysis interval, which improves the recovery efficiency.

4. DISCUSSION

The co-pyrolysis of oil shale and tar-rich coal is significant for the in-situ synchronized mining of both. The pyrolysis intervals of oil shale and tar-rich coal are the same, which makes it possible to synchronize the in-situ exploitation of both. The addition of tar-rich coal greatly enhances the pyrolysis characterization index of oil shale, especially in the air atmosphere. In addition, the co-pyrolysis of both did not adversely affect the pyrolysis oil quality. According to the principle of topical chemical reaction method [50], the co-pyrolysis of oil shale and tar-rich coal is the simultaneous exploitation of two resources, rather than the exploitation of one at the expense of the other [51]. The co-pyrolysis of both is not only in line with the characteristics of the two resources but also highly compatible with the topical chemical reaction method [52, 53]. The co-pyrolysis of both has a very high feasibility and development value [54].

5. CONCLUSIONS

Based on TG-DTG extrapolations, this paper presents the pyrolysis characterization and product analysis of Tongchuan oil shale, tar-rich coal, and their homogeneous mixture across three experimental conditions with varying pyrolysis atmospheres and heating rates, exploring the feasibility of simultaneous in-situ pyrolysis of both. The results show that in-situ co-pyrolysis of Tongchuan oil shale and tar-rich coal is highly feasible and exhibits strong adaptability to the topo-chemical situ reaction method. The specific conclusions are as follows:

- The thermogravimetric results of Tongchuan oil shale and tar-rich coal can be roughly divided into three stages. The

addition of tar-rich coal makes both achieve higher cracking degrees. In the air atmosphere, oxygenated gas occurs oxidative exothermic reaction with fixed carbon, which is important for triggering and maintaining the topical chemical reaction. Overall, oil shale and tar-rich coal are consistent in the major pyrolysis interval. This means that simultaneous extraction of both is possible.

- In a nitrogen atmosphere, the ignition temperature of T₃ was significantly lower than T₁, while the burnout temperature of T₃ was higher than T₁. The pyrolysis indexes of T₂ and T₃ were greater than T₁, with an increase of 50% and 40%, respectively. The pyrolytic stability of T₃ in the nitrogen atmosphere increased by about 66% compared to T₁. In the air atmosphere, a rapid heating rate leads to early condensation of tar and coking on the sample surface, resulting in a decrease in pyrolysis efficiency. The pyrolysis index of the comparative T₁ decreased from 4.2 times vs. 3.2 times to 2.4 times vs. 1.8 times.
- In the nitrogen atmosphere, the alkanes and olefins of T₃ showed a significant decrease. The contents of aromatic hydrocarbons and oxygenated compounds appeared to increase by 7.73% and 552.41%. The conversion of oxygenated compounds to phenolic compounds was inhibited at the rapid temperature increase of 20°C/min. The conversion of oxygenated compounds to phenolic compounds was inhibited at the rapid temperature increase of 20°C/min. A higher temperature increase rate promoted the interaction between free radicals and weakened the occurrence of secondary pyrolysis. In the air atmosphere, the content of oxygenated compounds increased the most, with a rise of 485.44%. The decrease of aromatic hydrocarbons was 17.97%. The oxidation reaction facilitated rapid oxidization of the sample, and the air atmosphere introduced excessive oxygenated groups for the pyrolysis reaction.

ACKNOWLEDGEMENTS

This research was funded by the National Key R&D Program of China (Grant No. 2019YFA0705501), the Young and Middle-aged Excellent Team Project for Scientific and Technological Innovation of Jilin Province of China (Grant No. 20220508135RC), the Independent Innovation Capacity Project of Jilin Province Development and Reform Commission (Grant No. 2022C021) the Program for JLU Science and Technology Innovative Research Team (Grant No. 2020TD-05), Study on the Mechanism of Oil Storage in Tongchuan Oil Shale and Key Parameters of In-situ Conversion (194-C-QT-2023-06-003), and Study on Key Technology and Equipment for Electric Heating in Long-Life Wells for In-situ Oil Shale Extraction (Grant No. 20240304162SF).

REFERENCES

- [1] P.C. Storch and L. Stamford, "Net zero in the heating sector: Technological options and environmental sustainability from now to 2050," *Energy Convers. Manage.*, vol. 230, no. 3, p. 113838, Feb. 2021, doi: [10.1016/j.enconman.2021.113838](https://doi.org/10.1016/j.enconman.2021.113838).

Feasibility study on in-situ heat injection of Tongchuan oil shale and tar-rich coal based on TG-DTG

- [2] W. He, Y. Sun, and X. Shan, "Organic matter evolution in pyrolysis experiments of oil shale under high pressure: Guidance for in situ conversion of oil shale in the Songliao basin," *J. Anal. Appl. Pyrolysis*, vol. 155, no. 6, p. 105091, May 2021, doi: [10.1016/j.jaap.2021.105091](https://doi.org/10.1016/j.jaap.2021.105091).
- [3] Q. Bu, Q. Li, and X. Li, "Numerical heat transfer simulation of oil shale large-size downhole heater," *Appl. Sci.*, vol. 14, no. 6, p. 2235, Mar. 2024, doi: [10.3390/app14062235](https://doi.org/10.3390/app14062235).
- [4] Z. Wang *et al.*, "Economic and heating efficiency analysis of double-shell downhole electric heater for tar-rich coal in-situ conversion," *Case Stud. Therm. Eng.*, vol. 41, p. 102596, Jan. 2023, doi: [10.1016/j.csite.2022.102596](https://doi.org/10.1016/j.csite.2022.102596).
- [5] Z.Y. Yu *et al.*, "In-situ infrared and kinetic characteristics analysis on pyrolysis of tar-rich coal and macerals," *Fuel*, vol. 348, p. 128601, Sep. 2023, doi: [10.1016/j.fuel.2023.128601](https://doi.org/10.1016/j.fuel.2023.128601).
- [6] Y. Ju, Y. Zhu, Y. Zhang, H. Zhou, S. Peng, and S. Ge, "Effects of high-power microwave irradiation on tar-rich coal for realising in situ pyrolysis, fragmentation, and low-carbon utilisation of tar-rich coal," *Int. J. Rock Mech. Mining Sci.*, vol. 157, p. 105165, Sep. 2022, doi: [10.1016/j.ijrmms.2022.105165](https://doi.org/10.1016/j.ijrmms.2022.105165).
- [7] B. Zhang, D. Kang, S. Ma, W. Duan, and Y. Zhang, "Densification and fracture type of desert in tight oil reservoirs: A case study of the Fuyu tight oil reservoir in the Sanzhao depression, Songliao basin," *Lithosphere*, vol. 2021, no. 4, p. 2609923, Jul. 2021, doi: [10.2113/2021/2609923](https://doi.org/10.2113/2021/2609923).
- [8] Y. Sun, L. He, S. Kang, W. Guo, Q. Li, and S. Deng, "Pore evolution of oil shale during sub-critical water extraction," *Energies*, vol. 11, no. 4, p. 842, Apr. 2018, doi: [10.3390/en11040842](https://doi.org/10.3390/en11040842).
- [9] S. Si *et al.*, "Oil charging power simulation and tight oil formation of Fuyu oil layer in Sanzhao area, Songliao basin," *Front. Earth Sci.*, vol. 10, p. 825548, Apr. 2022, doi: [10.3389/feart.2022.825548](https://doi.org/10.3389/feart.2022.825548).
- [10] X. Pang *et al.*, "Main controlling factors and movability evaluation of continental shale oil," *Earth-Sci. Rev.*, vol. 243, p. 104472, Aug. 2023, doi: [10.1016/j.earscirev.2023.104472](https://doi.org/10.1016/j.earscirev.2023.104472).
- [11] C. Er *et al.*, "Relationship between tight reservoir diagenesis and hydrocarbon accumulation: An example from the early Cretaceous Fuyu reservoir in the Daqing oil field, Songliao basin, China," *J. Pet. Sci. Eng.*, vol. 208, p. 109422, Jan. 2022, doi: [10.1016/j.petrol.2021.109422](https://doi.org/10.1016/j.petrol.2021.109422).
- [12] F. Yang *et al.*, "Thermodynamic analysis of in situ underground pyrolysis of tar-rich coal: primary reactions," *ACS Omega*, vol. 8, no. 21, pp. 18915–18929, May 2023, doi: [10.1021/acsomega.3c01321](https://doi.org/10.1021/acsomega.3c01321).
- [13] W. Xu *et al.*, "Evolution of organic carbon isotopes during the pyrolysis of Nongan oil shale in Songliao basin and its implications for in-situ conversion project," *Geomech. Geophys. Geo-Energy Geo-Res.*, vol. 9, no. 1, p. 65, Dec 2023, doi: [10.1007/s40948-023-00616-1](https://doi.org/10.1007/s40948-023-00616-1).
- [14] L. Ma *et al.*, "Investigation of pyrolysis and mild oxidation characteristics of tar-rich coal via thermogravimetric experiments," *ACS Omega*, vol. 7, no. 29, pp. 25613–25624, Jul 2022, doi: [10.1021/acsomega.2c02786](https://doi.org/10.1021/acsomega.2c02786).
- [15] Z. Miao, G. Wu, P. Li, X. Meng, and Z. Zheng, "Investigation into co-pyrolysis characteristics of oil shale and coal," *J. Mining Sci. Technol.*, vol. 22, no. 2, pp. 245–249 Mar 2012, doi: [10.1016/j.ijmst.2011.09.003](https://doi.org/10.1016/j.ijmst.2011.09.003).
- [16] P. Dong *et al.*, "Resource utilization of cyanide tailings: preparation of ferrous oxalate by a combined technique of anaerobic roasting-persulfate leaching followed by oxalic acid precipitation," *JOM*, vol. 76, pp. 432–444, 2024.
- [17] C. Jia, J. Chen, J. Bai, Y. Xun, S. Song, and Q. Wang, "Kinetics of the pyrolysis of oil sands based upon thermogravimetric analysis," *Thermochim. Acta*, vol. 666, pp. 66–74, Aug 2018, doi: [10.1016/j.tca.2018.06.002](https://doi.org/10.1016/j.tca.2018.06.002).
- [18] M. Citiroglu, E. Putun, G.D. Love, C.J. Lafferty, and C.E. Snapet, "Effect of lignite addition and steam on the pyrolysis of Turkish oil shales," *Fuel*, vol. 71, no. 12, pp. 1511–1514, Dec. 1992, doi: [10.1016/0016-2361\(92\)90227-F](https://doi.org/10.1016/0016-2361(92)90227-F).
- [19] Y. Xiong, M.A. Mingjie, and D. Zhao, "Pyrolysis features of oil shale from yaojie and the pyrolysate analysis," *Acta Pet. Sin.*, vol. 31, pp. 98–103, 2015, doi: [10.3969/j.issn.1001-8719.2015.01.016](https://doi.org/10.3969/j.issn.1001-8719.2015.01.016).
- [20] Q. Wang, C. Jia, and H. Liu, "Combustion kinetic model of Wangqing oil shale," *Zhongguo Dianji Gongcheng Xuebao/Proc. Chinese Society of Electrical Engineering*, vol. 32, no. 23, pp. 27–31, 2012.
- [21] F. Bai *et al.*, "Kinetic study on the pyrolysis behavior of Huadian oil shale via non-isothermal thermogravimetric data," *Fuel*, vol. 146, pp. 111–118, Apr. 2015, doi: [10.1016/j.fuel.2014.12.073](https://doi.org/10.1016/j.fuel.2014.12.073).
- [22] S. Zhao, Y. Sun, X. Lu, and Q. Li, "Energy consumption and product release characteristics evaluation of oil shale non-isothermal pyrolysis based on TG-DSC," *J. Pet. Sci. Eng.*, vol. 187, p. 106812, Apr. 2020, doi: [10.1016/j.petrol.2019.106812](https://doi.org/10.1016/j.petrol.2019.106812).
- [23] J. Bao, T. Jyun Syung, and B. Reza, "A review of the current progress of CO₂ injection EOR and carbon storage in shale oil reservoirs," *Fuel*, vol. 236, pp. 404–427, Jan. 2019, doi: [10.1016/j.fuel.2018.08.103](https://doi.org/10.1016/j.fuel.2018.08.103).
- [24] Y. Sun *et al.*, "Kinetic study of Huadian oil shale combustion using a multi-stage parallel reaction model," *Energy*, vol. 82, pp. 705–713, Mar. 2015, doi: [10.1016/j.energy.2015.01.080](https://doi.org/10.1016/j.energy.2015.01.080).
- [25] Y. Gao, T. Wan, Y. Dong, and Y. Li, "Numerical and experimental investigation of production performance of in-situ conversion of shale oil by air injection," *Energy Reports*, vol. 8, no. 8, pp. 15740–15753, Nov. 2022, doi: [10.1016/j.egyr.2023.01.119](https://doi.org/10.1016/j.egyr.2023.01.119).
- [26] Y. Sun *et al.*, "A novel energy-efficient pyrolysis process: self-pyrolysis of oil shale triggered by topochemical heat in a horizontal fixed bed," *Sci. Rep.*, vol. 5, p. 8290, Feb. 2015, doi: [10.1038/srep08290](https://doi.org/10.1038/srep08290).
- [27] S.T. Xu *et al.*, "Regulating the oxidative assisted pyrolysis of Huadian oil shale by preheating temperature and oxygen flow rate," *Energy*, vol. 262, p. 125602, Jan. 2023, doi: [10.1016/j.energy.2022.125602](https://doi.org/10.1016/j.energy.2022.125602).
- [28] W. Guo, Q. Li, S. Deng, Y. Wang, and C. Zhu, "Mechanism and reservoir simulation study of the autothermic pyrolysis in-situ conversion process for oil shale recovery," *Pet. Sci.*, vol. 20, no. 2, pp. 1053–1067, 2023, doi: [10.1016/j.petsci.2022.08.030](https://doi.org/10.1016/j.petsci.2022.08.030).
- [29] F. Bai, Y. Sun, Y. Liu, Q. Li, and M. Guo, "Thermal and kinetic characteristics of pyrolysis and combustion of three oil shales," *Energy Convers. Manage.*, vol. 97, pp. 374–381, Jun. 2015, doi: [10.1016/j.enconman.2015.03.007](https://doi.org/10.1016/j.enconman.2015.03.007).
- [30] Z. Hong *et al.*, "Establishment of combustion stability index of pulverized-coal," *J. Combust. Sci. Technol.*, vol. 9, no. 4, pp. 364–366, 2003, doi: [10.1007/BF0297489](https://doi.org/10.1007/BF0297489).
- [31] J. Zhao *et al.*, "Study on molecular structural heterogeneity of tar-rich coal based on micro-FTIR," *Spectrochim. Acta-Part A*, vol. 330, p. 125749, Apr. 2025, doi: [10.1016/j.saa.2025.125749](https://doi.org/10.1016/j.saa.2025.125749).
- [32] T. Xu, Y. Lei, L. Chen, and Y. Wu, "Thermal properties and grey

- correlation degree analysis of tar-rich coal under cryogenic and pyrolysis condition,” *Fuel*, vol. 371, p. 132170, Sep. 2024, doi: [10.1016/j.fuel.2024.132170](https://doi.org/10.1016/j.fuel.2024.132170).
- [33] Z. Wang *et al.*, “Studies on the co-pyrolysis characteristics of oil shale and spent oil shale,” *J. Therm. Anal. Calorim.*, vol. 123, no. 2, pp. 1707–1714, Feb. 2016, doi: [10.1007/s10973-015-5012-3](https://doi.org/10.1007/s10973-015-5012-3).
- [34] F. Liu *et al.*, “Hydrocarbon regulation and lower temperature pyrolysis of balikun oil shale kerogen,” *Energy & Environment*, vol. 35, no. 2, pp. 597–609, Mar. 2024, doi: [10.1177/0958305x221133263](https://doi.org/10.1177/0958305x221133263).
- [35] W. Guo, J. Pan, Q. Yang, Q. Li, S. Deng, and C. Zhu, “Study of the residual carbon oxidation trigger mechanism in fractured oil shale formation under real condition,” *Int. Commun. Heat Mass Transfer*, vol. 160, p. 108369, Jan. 2025, doi: [10.1016/j.icheatmasstransfer.2024.108369](https://doi.org/10.1016/j.icheatmasstransfer.2024.108369).
- [36] W. Guo, C. Fan, S. Deng, H. Shui, and Z. Liu, “Secondary cracking characteristics of asphaltenes and insights into the reservoir unblocking during oil shale in-situ exploitation,” *Adv. Geo-Energy Res.*, vol. 15, no. 1, pp. 13–26, Jan. 2025, doi: [10.46690/ager.2025.01.03](https://doi.org/10.46690/ager.2025.01.03).
- [37] S. Xu *et al.*, “Optimization of temperature parameters for the autothermic pyrolysis in-situ conversion process of oil shale,” *Energy*, vol. 264, p. 126309, Feb. 2023, doi: [10.1016/j.energy.2022.126309](https://doi.org/10.1016/j.energy.2022.126309).
- [38] J. Lei *et al.*, “A comprehensive analysis of the pyrolysis effects on oil shale pore structures at multiscale using different measurement methods,” *Energy*, vol. 227, p. 120359, Jul. 2021, doi: [10.1016/j.energy.2021.120359](https://doi.org/10.1016/j.energy.2021.120359).
- [39] S. Deng, Z. Wang, Q. Gu, F. Meng, J. Li, and H. Wang, “Extracting hydrocarbons from Huadian oil shale by sub-critical water,” *Fuel Process. Technol.*, vol. 92, no. 5, pp. 1062–1067, May 2011, doi: [10.1016/j.fuproc.2011.01.001](https://doi.org/10.1016/j.fuproc.2011.01.001).
- [40] J. Gu, S. Deng, Y. Sun, W. Guo, H. Chen, and B. Shi, “Pyrolysis behavior and pyrolysate characteristics of Huadian oil shale kerogen catalyzed by nickel-modified montmorillonite,” *Adv. Geo-Energy Res.*, vol. 11, no. 3, pp. 168–180, Mar. 2024, doi: [10.46690/ager.2024.03.02](https://doi.org/10.46690/ager.2024.03.02).
- [41] Y. Jia *et al.*, “Catalytic pyrolysis of tar-rich coal for coal tar to light oil with catalysts of modified granulated blast furnace slag,” *J. Therm. Anal. Calorim.*, vol. 149, no. 8, pp. 3097–3110, Apr. 2024, doi: [10.1007/s10973-024-12932-z](https://doi.org/10.1007/s10973-024-12932-z).
- [42] W. Guo *et al.*, “Enhanced pyrolysis of Huadian oil shale at high temperature in the presence of water and air atmosphere,” *J. Pet. Sci. Eng.*, vol. 215, p. 110623, Aug. 2022, doi: [10.1016/j.petrol.2022.110623](https://doi.org/10.1016/j.petrol.2022.110623).
- [43] H. Jiang *et al.*, “Effect of hydrothermal pretreatment on product distribution and characteristics of oil produced by the pyrolysis of Huadian oil shale,” *Energy Convers. Manage.*, vol. 143, pp. 505–512, Jul. 2017, doi: [10.1016/j.enconman.2017.04.037](https://doi.org/10.1016/j.enconman.2017.04.037).
- [44] S. Xu *et al.*, “Regulating the oxidative assisted pyrolysis of Huadian oil shale by preheating temperature and oxygen flow rate,” *Energy*, vol. 262, p. 125602, Jan. 2023, doi: [10.1016/j.energy.2022.125602](https://doi.org/10.1016/j.energy.2022.125602).
- [45] X. Ning, X. Huang, X. Xue, C. a. Wang, L. Deng, and D. Che, “Experimental study on yield and quality of tar from tar-rich coal under the simulated in-situ conditions,” *J. Energy Inst.*, vol. 118, p. 101912, Feb. 2025, doi: [10.1016/j.joei.2024.101912](https://doi.org/10.1016/j.joei.2024.101912).
- [46] Z. Chang, C. Wang, W. Kuang, Y. Tang, X. Wu, and S. Liu, “Product characterization and pore structure evolution of a tar-rich coal following pyrolysis under nitrogen, steam/nitrogen, and oxygen nitrogen atmospheres,” *J. Anal. Appl. Pyrolysis*, vol. 180, p. 106563, Jun. 2024, doi: [10.1016/j.jaap.2024.106563](https://doi.org/10.1016/j.jaap.2024.106563).
- [47] J. Gu *et al.*, “Pyrolysis characteristics and evolution of the organics in Nong’an oil shale lump during sub-critical water extraction,” *Fuel*, vol. 364, p. 131064, May 2024, doi: [10.1016/j.fuel.2024.131064](https://doi.org/10.1016/j.fuel.2024.131064).
- [48] J. Han, Y. Sun, W. Guo, Q. Li, and S. Deng, “Characterization of pyrolysis of nong’an oil shale at different temperatures and analysis of pyrolysate,” *Oil Shale*, vol. 36, no. 2, pp. 151–170, 2019, doi: [10.3176/oil.2019.2S.06](https://doi.org/10.3176/oil.2019.2S.06).
- [49] X. Zhang, W. Guo, J. Pan, C. Zhu, and S. Deng, “In-situ pyrolysis of oil shale in pressured semi-closed system: Insights into products characteristics and pyrolysis mechanism,” *Energy*, vol. 286, p. 129608, Jan. 2024, doi: [10.1016/j.energy.2023.129608](https://doi.org/10.1016/j.energy.2023.129608).
- [50] W. Guo, S. Deng, and Y. Sun, “Recent advances on shale oil and gas exploration and development technologies,” *Adv. Geo-Energy Res.*, vol. 11, no. 2, pp. 81–87, Feb. 2024, doi: [10.46690/ager.2024.02.01](https://doi.org/10.46690/ager.2024.02.01).
- [51] H. Jiang *et al.*, “Preliminary Study on Copyrolysis of Spent Mushroom Substrate as Biomass and Huadian Oil Shale,” *Energy Fuels*, vol. 30, no. 8, pp. 6342–6349, Aug. 2016, doi: [10.1021/acs.energyfuels.6b01085](https://doi.org/10.1021/acs.energyfuels.6b01085).
- [52] W. Guo *et al.*, “Experimental study of the autothermic pyrolysis in-situ conversion process (ATS) for oil shale recovery,” *Energy*, vol. 258, p. 124878, Nov. 2022, doi: [10.1016/j.energy.2022.124878](https://doi.org/10.1016/j.energy.2022.124878).
- [53] C. Zhu *et al.*, “Reaction mechanism and reservoir simulation study of the high-temperature nitrogen injection in-situ oil shale process: A case study in Songliao Basin, China,” *Fuel*, vol. 316, p. 123164, May 2022, doi: [10.1016/j.fuel.2022.123164](https://doi.org/10.1016/j.fuel.2022.123164).
- [54] Z. Yu *et al.*, “Kinetic characteristics and product distribution of tar-rich coal in-situ underground pyrolysis: Influence of heterogeneous coal seam,” *J. Anal. Appl. Pyrolysis*, vol. 183, p. 106729, Oct. 2024, doi: [10.1016/j.jaap.2024.106729](https://doi.org/10.1016/j.jaap.2024.106729).